

Rotation and activity in the solar-metallicity open cluster NGC 2516^{1,2}

Donald M. Terndrup³ and Marc Pinsonneault

*Department of Astronomy, Ohio State University, 140 West 18th Avenue, Columbus, OH
43210*

terndrup@astronomy.ohio-state.edu, pinsono@astronomy.ohio-state.edu

Robin D. Jeffries and Alison Ford⁴

Department of Physics, Keele University, Keele, Staffordshire ST5 5BG, United Kingdom

rdj@astro.keele.ac.uk, Alison.Ford@open.ac.uk

John R. Stauffer³

*Infrared Processing and Analysis Center, California Institute of Technology, Mail Code
100-22, 770 South Wilson Avenue, Pasadena, CA 91125*

stauffer@ipac.caltech.edu

and

Alison Sills

*Department of Physics and Astronomy, McMaster University, 120 Main Street West,
Hamilton, Ontario L8S 4M1, Canada*

asills@mcmail.cis.mcmaster.ca

ABSTRACT

¹Based on observations obtained at the Anglo-Australian Telescope.

²Based on observations obtained at the Cerro Tololo-Interamerican Observatory, NOAO, which is operated by the Associated Universities for Research in Astronomy (AURA), Inc., under cooperative agreement with the National Science Foundation.

³Visiting Astronomer, Cerro Tololo Inter-American Observatory, NOAO.

⁴Present address, Physics and Astronomy Group, The Open University, Walton Hall, Milton Keynes MK7 6AA, United Kingdom.

We report new measures of radial velocities and rotation rates ($v \sin i$) for 51 F and early-G stars in the open cluster NGC 2516, and combine these with previously published data. From high signal-to-noise spectra of two stars, we show that NGC 2516 has a relative iron abundance with respect to the Pleiades of $\Delta[\text{Fe}/\text{H}] = +0.04 \pm 0.07$ at the canonical reddening of $E(B - V) = 0.12$, in contrast to previous photometric studies that placed the cluster 0.2 to 0.4 dex below solar. We construct a color-magnitude diagram based on radial velocity members, and explore the sensitivity of photometric determinations of the metallicity and distance to assumed values of the reddening. For a metal abundance near solar, the Hipparcos distance to NGC 2516 is probably underestimated. Finally, we show that the distribution of rotation rates and X-ray emission does not differ greatly from that of the Pleiades, when allowance is made for the somewhat older age of NGC 2516.

Subject headings: open clusters and associations: individual (NGC 2516) — stars: distances — stars: rotation — Xrays: stars

1. Introduction

Observations of stellar rotation rates in young clusters demonstrate that stars must lose a considerable fraction of their initial angular momentum both before and after arrival on the main sequence. In young clusters such as Alpha Persei (age ~ 50 Myr) or the Pleiades (age ~ 100 Myr), stars at any mass are seen to rotate at a variety of rates (e.g., Stauffer, Hartmann, & Jones 1989; Queloz et al. 1999; Terndrup et al. 2000), with most rotating slowly ($v \sin i \leq 10 - 15 \text{ km s}^{-1}$), but a minority rotating much more quickly ($v \sin i \geq 30 \text{ km s}^{-1}$). By the age of the Hyades (600 Myr), all but the lowest-mass stars have spun down to slow rotation rates (Radick et al. 1987; Stauffer, Hartmann, & Latham 1987; Jones, Fischer, & Stauffer 1996; Terndrup et al. 2000; Tinker, Pinsonneault, & Terndrup 2002). This picture is reinforced by observations in clusters with ages between the Pleiades and the Hyades, such as M 34 = NGC 1039 (Soderblom, Jones, & Fischer 2001) or NGC 6475 (James & Jeffries 1997), although in these clusters the number of stars with measured rotation rates is smaller than in the more well-studied systems. Here and throughout this paper, ages come from Meynet, Mermilliod, & Maeder (1993), unless otherwise stated; we do not use ages derived from the “lithium depletion boundary” technique (Stauffer, Shultz, & Kirkpatrick 1998; Barrado y Navascués, Stauffer, & Patten 1999; Stauffer et al. 1999), because few clusters have ages measured in this manner.

The current evolutionary paradigm for stellar angular momentum loss has a number

of ingredients that are motivated by observations or theory. The main sequence spindown is attributed to magnetic coupling between the stellar envelope and an ionized wind (e.g., Schatzman 1962; Weber & Davis 1967), which would cause a star to spin down over tens to hundreds of millions of years. The existence of rapid rotators in clusters of age < 200 Myr requires that the angular momentum loss rate must be suppressed or saturated at high rotation rates (Kawaler 1988; MacGregor & Brennan 1991). The presence of slow rotators in young clusters points to an additional loss mechanism acting over lifetimes of a few Myr (Cameron & Campbell 1993; Keppens, MacGregor, & Charbonneau 1995); motivated by the theoretical work of Königl (1991) and Shu et al. (1994), which showed that magnetic torques can transfer angular momentum away from a protostar onto its accretion disk, this early loss is termed “disk locking.”

Much of the effort to understand the evolution of spin rates has concentrated on using clusters of various ages to set constraints on the duration of disk-locking and mass-dependence of saturation used in the models (Krishnamurthi et al. 1997; Allain 1998; Sills, Pinsonneault, & Terndrup 2000). An important but often unstated assumption in many of these studies is that open clusters of different ages sample a single time sequence of angular momentum loss. For this to be the case, the distribution of initial specific angular momenta and disk locking lifetimes, as well as the properties of saturation and of winds, would be the same in all open clusters (specifically, the dependence on stellar mass would be identical). Testing this assumption has always been difficult since most of the available data were for Alpha Persei, the Pleiades, and the Hyades, which mainly sample the loss mechanisms on the main sequence. Consequently there have been a number of efforts underway to obtain new observations of more clusters of similar age (e.g., Jones et al. 1997; James & Jeffries 1997), or by extending observations to very young systems such as the Orion Nebula Cluster (Attridge & Herbst 1992; Stassun et al. 1999; Herbst et al. 2000; Herbst, Bailer-Jones, & Mundt 2001; Rebull 2001). Recently, Tinker, Pinsonneault, & Terndrup (2002) have shown that a single set of parameters describing the angular momentum loss can explain the rotational evolution from Orion to the Pleiades and Hyades.

The southern open cluster NGC 2516 provides an important additional laboratory for exploring the evolution of angular momentum in young clusters. NGC 2516 is a fairly rich cluster with a mass about twice that of the Pleiades, in which many possible members have been identified photometrically (Jeffries, Thurston, & Hambly 2001). There have been radial velocity studies of bright stars near the main-sequence turnoff (González & Lapasset 2000), and a previous study of the rotation rates of F-G stars (Jeffries, James & Thurston 1998) which we extend in this paper. The cluster has also been the target of several X-ray surveys (Jeffries, Thurston, & Pye 1997; Micela et al. 2000; Harnden et al. 2001; Sciortino et al. 2001), and has a distance determination from Hipparcos parallaxes (Robichon et al. 1999).

NGC 2516 has been of particular interest because several previous photometric studies have suggested a low metallicity, a few tenths dex below solar (Cameron 1985; Jeffries, Thurston, & Pye 1997; Jeffries, James & Thurston 1998; Pinsonneault et al. 1998). In contrast, a preliminary metallicity estimate from an equivalent width analysis of relatively low signal-to noise spectra (Jeffries, James & Thurston 1998) indicated an abundance for NGC 2516 that was solar within the errors. As in any other cluster, the cluster age from the main-sequence turnoff depends sensitively on the metallicity. If NGC 2516 is near solar metallicity, it has an age of 140 Myr, but would have an age about 180 Myr for $[{\rm Fe/H}] \approx -0.3$, a difference of 30%. Furthermore, accurate age determinations enter into many other aspects of stellar evolution in open clusters, such as the relation between the initial and final masses of white dwarfs and the maximum mass of white dwarf progenitors (Koester & Reimers 1996; Jeffries 1997; von Hippel & Gilmore 2000; Weidemann 2000).

Determining the metallicity of NGC 2516 is also critical for using the cluster as a probe of the metallicity dependence of angular momentum loss. Theory shows that, once on the main sequence, the depth of the outer convective zone depends mainly on stellar mass, somewhat on metallicity, and hardly at all on stellar age (e.g., Pinsonneault, DePoy, & Coffee 2001). Stars of low metallicity have shallower convective zones at a given effective temperature, and because low-metallicity stars of a given mass are also hotter and less luminous than their solar-abundance counterparts, their convection zones should be thinner than higher-abundance stars of the same color.

Here we present the results of a spectroscopic study of NGC 2516, which combines parallel efforts led by two of us (DMT and RDJ). In § 2, we discuss the observations and data reduction, and proceed in § 3 to derive a metallicity for NGC 2516 both from new spectra and from analysis of the color-magnitude diagram. In § 4, we discuss the rotational properties of the stars in our combined sample, and present our conclusions in § 5.

2. Observations and Data Reduction

2.1. Photometry

Photometry comes from a new catalog prepared by Jeffries, Thurston, & Hambly (2001) from a CCD survey of 0.86 square degree of NGC 2516, obtained at the CTIO 0.9-m telescope during three nights in January 1995. Conditions were photometric and the individual CCD frames were flat-fielded with twilight exposures. Nightly corrections for extinction and transformations to the Johnson V , $B - V$ and Cousins $V - I_C$ systems were achieved using many observations of standard fields from the Landolt (1992) compilation. The numbers of

standards observed ensures that, for stars of the colors considered in this paper, statistical errors in transforming to the standard colors and magnitudes can be neglected.

Aperture photometry was performed using small apertures (either 3 or 6 arcsec radius) on a series of 25 mosaicked CCD fields, each covering an area of 13.5×13.5 arcminutes² at a scale of 0.4 arcsec/pixel. Comparison of stars in the overlapping regions of the CCD fields gives us a good idea of the internal photometry errors. For the stars considered in this paper, with $V = 11 - 15$, these internal errors are 0.022 mag in V , and 0.015 mag in $B - V$ and $V - I_C$. Residuals to the linear transformation functions used to fit the Landolt standards were less than 0.02 mag on all nights.

2.2. Spectroscopy at Cerro Tololo

Most of our new spectra were obtained in two runs at the Blanco 4 m telescope at Cerro Tololo in March 1998 and January 1999. For both runs, we used the echelle spectrograph with “red long” camera to produce spectra with an average dispersion of $\approx 0.08 \text{ \AA pixel}^{-1}$. The effective resolution as measured from the FWHM of arc lamp lines was 2.4 pixels, or 8.7 km s^{-1} at $\text{H}\alpha$. The spectra taken in 1998 used the G181 cross disperser (316 l mm^{-1}), and covered the wavelength interval $5840 - 8150 \text{ \AA}$ in 28 orders. In 1999, we used the 226-3 cross disperser (226 l mm^{-1}) to obtain spectra from 5180 \AA to 8280 \AA in 39 orders. The wavelength coverage in each order exceeded the free spectral range, so the wavelengths at the ends of each order were sampled twice. In each run, we obtained spectra of bright field stars with known radial velocity spanning the temperature range of our NGC 2516 targets, and took spectra of the evening twilight sky. Most of the spectra from CTIO have signal-to-noise of 15-25 per resolution element, but we obtained repeated long exposures of two stars for an abundance analysis of NGC 2156, below.

Basic image processing and spectral reductions were performed with scripts written for the IRAF⁵ and VISTA packages (Stover 1998). After removal of the overscan level and a zero-exposure frame, each image was processed with a moving-box median filtering algorithm to remove the many cosmic rays. The spectral orders were then traced using the exposures of bright stars, and the sky and object apertures were defined for each object to maximize the number of pixels contributing to the sky. Finally, the spectra were extracted using an unweighted sum over the spectral aperture after background subtraction. This background subtraction also removed scattered light from the spectra.

⁵IRAF is distributed by the National Optical Astronomy Observatory, operated by AURA, Inc., under cooperative agreement with the National Science Foundation.

The spectrograph at CTIO exhibits considerable flexure with telescope position, amounting to ± 1.5 pixels at the declination of NGC 2516 during each night. We corrected for this by cross correlating selected orders of the extracted spectra containing the A and B atmospheric bands, and then applied the measured pixel shifts to bring each spectrum to a uniform zero point. The accuracy of this process was estimated by the scatter in the derived pixel shifts for the four orders that had significant telluric absorption. The average error was typically 0.1 pixel, which is equivalent to 0.36 km s^{-1} at $\text{H}\alpha$, but was occasionally higher. This error was later added in quadrature to the error in the radial velocity.

Wavelength calibration was achieved using ThAr lamp spectra in two steps. In the first, lines were identified and a trial solution was obtained independently for each order. In the second step, quadratic polynomials were fit to the central wavelength and dispersion as a function of order number, and the line identifications and solutions for the wavelength at each pixel were rederived using this fit as a starting point. In this step, as before, each order had an independent wavelength solution.

Radial velocities were measured by cross correlation of seven extracted orders of each spectra against the equivalent orders of bright, high signal-to-noise template stars in the lists of Udry, Mayor, & Queloz (1999) and Stefanik, Latham, & Torres (1999). The seven orders were chosen to have many stellar absorption features and to be relatively free of telluric absorption, and had central wavelengths from 6040 \AA to 6778 \AA . Each order was separately cross correlated and the results averaged. The scatter in the velocities for the separate orders was used to estimate the error in the velocity. The lowest velocity errors, about 0.5 km s^{-1} , were found for the most narrow-lined stars (i.e., the most slowly rotating ones) and/or those stars with higher signal to noise. For stars of moderate to rapid rotation, the radial velocity error is typically about $1/20$ the value of $v \sin i$. The total error was taken as the quadrature sum of the radial velocity error and the error in the flexure correction. The average error for the entire sample was about 1.1 km s^{-1} .

The zero point of the radial velocity system was defined by the stars HR 2593 (spectral type K2), HR 4540 (F8), HR 4695 (K1), and HR 5353 (G5). The estimated external error for the velocities in this system is 0.4 km s^{-1} .

The width of the cross correlation between each star and the template was used to determine the rotational velocity. The calibration of the relation between the correlation widths and $v \sin i$ was determined by convolving the spectrum of another high signal-to-noise spectrum of a slowly-rotating star with rotational broadening functions, then cross-correlating those artificially broadened spectra with the template star spectrum (cf. Hartmann et al. 1986). The broadening functions are given by Gray (1992); we adopted a limb-darkening coefficient $\epsilon = 0.6$.

2.3. Spectroscopy at the AAT

Data were taken on the AAT on 2000 February 23-24. The UCL Echelle Spectrograph with 79 lines mm^{-1} grating was used at the Coudé focus, with a MITLL3 chip. The central wavelength was 6150Å in order 37. A 1.2'' slit was used, giving a resolution of 0.13Å at 0.036Å pixel $^{-1}$ (in order 33).

The data were reduced at the Keele Starlink node, using the ECHOMOP, FIGARO and UCLSYN packages (Mills, Webb & Clayton 1997; Smith 1992). As with the CTIO data, the spectra reduction here included background subtraction (including scattered light), and wavelength calibration.

Radial velocities were measured using cross-correlation techniques in the spectral range 5210-5340Å and 5460-5600Å, which contain many neutral metal lines. The standard templates used to determine heliocentric RVs were radial velocity standards HR 1829 (G5 V) and HR 4540 (F9 V). Internal errors are dominated by small shifts in the wavelength calibrations during exposures amounting to about 1 km s $^{-1}$. External errors, found by comparing standard star observations, are estimated to be 0.4 km s $^{-1}$.

Rotational velocities were obtained by fitting a synthetic spectrum to the data, allowing the line abundances and rotational velocity to vary until the minimum χ^2 value was obtained. The atmospheres used were those of Kurucz (1993) and used a mixing length approximation with no overshooting. Oscillator strengths were fixed by comparison with a solar spectrum taken with the same instrumentation.

The spectral range used was 5260-5290Å, which was in the order with the deepest lines. Temperatures for the synthesis were calculated from the $B - V$ photometry given in the catalog of Jeffries, Thurston, & Hambly (2001), using the prescription of Saxner & Hammarbäck (1985), which includes a dependence on [Fe/H]. For this analysis, we assumed [Fe/H] = -0.32, but the results would be nearly the same had we assumed solar abundance.⁶ Errors in $v \sin i$ were obtained by finding the $v \sin i$ at which the χ^2 values increased by an amount appropriate for the number of degrees of freedom. This was added in quadrature to an uncertainty of around 0.7 km s $^{-1}$, which arises from uncertainties in the effective temperature put into the synthesis (a change in $B - V$ of 0.02 changes the temperature by 75 K at 6500 K).

⁶The metallicity of the atmosphere used in the analysis has little effect on the line widths, but would change the relation between color and effective temperature. Adopting solar metallicity would have made the models ≈ 100 K hotter. The difference in the intrinsic width of the lines for this temperature change does not produce a significant effect in the derived value of $v \sin i$.

2.4. Results and internal checks

Table 1 presents our measurements in NGC 2516. Column 1 lists the name of each star, where DK indicates the list of Dachs & Kabus (1989), E indicates Eggen (1972), and the remaining names are from the photometric catalog of Jeffries, Thurston, & Hambly (2001) or those used in Jeffries, James & Thurston (1998). Columns 2 – 6 display the source for the data, the radial velocity and its error, and the rotational velocity and its error. Finally, the last five columns show the photometry, catalog entry, and a photometric membership flag for each star from Jeffries, Thurston, & Hambly (2001). The first part of the table shows stars which we class as cluster members because their radial velocities are statistically consistent with the cluster mean velocity, while the second part shows stars with discrepant radial velocities. These memberships were assigned by an iterative scheme that determined which stars were within 3σ of the cluster mean velocity. We determined the mean by combining our observations here with the velocities for members in Jeffries, James & Thurston (1998). The reported errors were increased by adding 1 km s^{-1} in quadrature to account for the likely velocity dispersion in the cluster (Stauffer et al. 1997).

Six of the stars in the CTIO sample had previously been observed by Jeffries, James & Thurston (1998). The weighted mean difference in radial velocity in the sense (CTIO – previous) is $+1.1 \text{ kms}$, indicating that the CTIO data have a slightly higher zero point in velocity than the earlier work. The weighted scatter in the difference is 0.9 km s^{-1} , where a value of 1.3 km s^{-1} would be the expected error from the random errors in the velocities. Table 2 lists the mean cluster velocity from this study and earlier works; the error in that table includes only random errors. The mean velocity for our full sample is slightly higher than derived in Jeffries, James & Thurston (1998), but is not statistically significant given the external errors here and that paper ($\approx 0.4 \text{ km s}^{-1}$). Our cluster velocity is distinctly greater than the value of $+19 \text{ km s}^{-1}$ quoted in the Lyngå (1987) catalog, and is somewhat greater than the value of $22.0 \pm 0.2 \text{ km s}^{-1}$ derived for early-type stars and red giants in NGC 2516 by González & Lapasset (2000). The latter study included a correction of -0.6 km s^{-1} for the gravitational redshift of main-sequence stars, a correction we do not apply here. Had we applied such a correction, our mean cluster velocity would still be slightly higher than in González & Lapasset (2000).

Figure 1 shows the correlation of the new and older values of $v \sin i$; the solid line on that figure indicates equality and is not a fit to the data points. Five of the stars agree within the errors, while one star (DK 206) has a $v \sin i$ value from CTIO that is considerably greater than found previously. We are unable to discern the source of this discrepancy, although we have verified that the recorded coordinates for this star on the CTIO run match the catalog position of DK 206.

All but two of the stars we observed were listed as probable members in Jeffries, Thurston, & Hambly (2001), where membership was determined by proximity to the main sequence in both the V , $B - V$ and V , $V - I$ color-magnitude diagrams and in the $B - V$, $V - I$ two-color plot. The exceptions are DK 573 and DK 742, which passed two of the tests.

Of the stars listed as non-members (lower part of Table 1), most are photometric members in Jeffries, Thurston, & Hambly (2001). Three of these (DK 417, DK 669, and DK 919) have velocities within 20 km s^{-1} of the cluster mean. Of these, only DK 417 has a detected rotational velocity ($v \sin i = 17.9 \text{ km s}^{-1}$), and so may be a binary member of NGC 2516. DK 669 is listed as a photometric binary candidate in Jeffries, Thurston, & Hambly (2001). Several other stars have more discrepant velocities but also exhibit significant rotation (DK 306, DK 503, and DK 508); these may be candidate short-period binaries. Of these three, only DK 508 is a binary candidate from photometry. Second-epoch radial velocities would be helpful to further elucidate their nature. To be conservative, we have not included the non-member stars in the discussion below.

3. Analysis

3.1. The abundance of NGC 2516

We obtained repeated, long exposures of two slowly-rotating stars (DK 320 and DK 325); the resulting average spectra are of sufficient quality (peak S/N of about 70 per pixel) to attempt a fine spectroscopic abundance analysis. From the point of view of open cluster studies, the best approach is to define the abundance relative to other well studied clusters such as the Pleiades. To do this, we performed a differential iron abundance analysis with respect to the Sun, using lines for which equivalent widths have been published for Pleiades stars. We analyzed our measured widths in NGC 2516 and those in the Pleiades using the same model atmospheres and adopted temperature scale.

We chose to work with a set of six isolated, unblended Fe I lines concentrated around 6700 \AA (specifically 6677 \AA , 6703 \AA , 6705 \AA , 6726 \AA , 6750 \AA , and 6752 \AA). Equivalent widths for these lines in a set of Pleiades F dwarfs are given by Boesgaard, Budge, & Burck (1988) and by Boesgaard, Budge, & Ramsay (1988). We found that many of the other lines employed by Boesgaard & Friel, specifically those with $\lambda > 7000 \text{ \AA}$, were blends, and that our measurements of line strengths in twilight solar spectra were not in agreement with the values quoted by Boesgaard & Friel.

We measured the equivalent widths of our chosen lines in both of the two targets and in a twilight solar spectrum using the same instrumentation and reduced in a similar way.

We compared the solar equivalent widths with those from the Kitt Peak Solar Atlas, finding good agreement in all cases. We then used the one-dimensional homogeneous LTE model ATLAS9 model atmospheres (Kurucz 1993) to calculate the iron abundances. The atmospheres incorporated the mixing length treatment of convection with $\alpha = 1.25$. We did this in a differential way with respect to the Sun, assuming solar parameters of $T_{\text{eff}} = 5777$ K, $\log g = 4.44$, and a microturbulent velocity of 1.0 km s^{-1} . The gf factors for the lines were tuned to give a solar iron abundance of 7.54 (Milford, O’Mara, & Ross 1994) on the usual logarithmic scale where the abundance of hydrogen is 12.

The equivalent widths for our target stars and for the Pleiades F stars were then fed into the same models with T_{eff} determined from $B - V$ via the Saxner & Hammarbäck (1985) relationship, assuming a solar metal abundance and $\log g = 4.5$. We assumed $E(B - V) = 0.12$ for NGC 2516 (Lyngå & Wramdemark 1984; Dachs & Kabus 1989) and $E(B - V) = 0.04$ for the Pleiades (Crawford & Perry 1976; Stauffer & Hartmann 1987) to obtain intrinsic colors. We allowed the microturbulence to be a fitting parameter, requiring that the derived iron abundance was independent of line equivalent width. We found that in all cases the microturbulence was in the range 1.0 to 1.75 km s^{-1} with an uncertainty of about 0.25 km s^{-1} . To investigate systematic errors, we re-determined abundances using different values of T_{eff} , $\log g$, and microturbulence. A temperature variation of ± 100 K, corresponding to a change in intrinsic color of ∓ 0.03 mag, led to $\Delta[\text{Fe/H}] = \pm 0.07$; a change in $\log g = \pm 0.2$ gave $\Delta[\text{Fe/H}] = \pm 0.03$; a change in the microturbulence of $+0.25 \text{ km s}^{-1}$ led to $\Delta[\text{Fe/H}] = \mp 0.04$.

We find $[\text{Fe/H}] = -0.02 \pm 0.03$ for DK 320 and $[\text{Fe/H}] = +0.13 \pm 0.04$ for DK 325, where the error is the standard error in the mean from the six lines. To these errors we add about 0.08 dex to account for errors in the photometry, gravity, and microturbulence. The mean for NGC 2516 from the two stars is therefore $[\text{Fe/H}] = +0.05 \pm 0.06$. To put this onto an absolute abundance scale we should then also have to consider errors in the assumed temperature scale, atmospheric models, and assumed mean reddening. We should also consider the consequences of using $[\text{Fe/H}] = 0$ to calculate the temperatures from the intrinsic colors. This is in fact a small correction, because each 0.1 dex decrease in metallicity only decreases the assumed effective temperature by ≈ 30 K. Thus if we had assumed initially that $[\text{Fe/H}] = -0.3$ for the purpose of calculating T_{eff} , we would have derived $[\text{Fe/H}] = -0.01$ from the spectra, which is clearly inconsistent with the original assumption.

There were six Pleiades stars for which all six Fe I lines had equivalent width measurements. We find a mean $[\text{Fe/H}] = 0.01 \pm 0.03$, assuming intrinsic color errors of ± 0.02 and assuming similar gravity and microturbulence errors to the NGC 2516 stars. This is in reasonable agreement with $[\text{Fe/H}] = -0.034 \pm 0.024$ found by Boesgaard & Friel (1990), who also employed the Saxner & Hammarbäck (1985) temperature scale in their analysis.

For the purposes of comparison, the ratio of iron abundance in NGC 2516 and the Pleiades does not depend on the adopted temperature scale nor on the model atmospheres employed, because both sets of data were treated in the same way.⁷ The logarithmic ratio of the iron abundances in NGC 2516 to the Pleiades is therefore $\Delta[\text{Fe}/\text{H}] = +0.04 \pm 0.07$, and so we therefore conclude that the metallicity of NGC 2516 is roughly solar abundance. For our final value, we combine this differential measurement of $[\text{Fe}/\text{H}]$ and the Boesgaard & Friel scale for the Pleiades and conclude that the metallicity of NGC 2516 is $[\text{Fe}/\text{H}] = +0.01 \pm 0.07$.

The only additional error is about ± 0.02 in $[\text{Fe}/\text{H}]$ for every ± 0.01 change in the relative reddening values for each cluster. We discuss the reddening in further detail in the next section when we look at the CMD for NGC 2516, but for now we note that if we took an extreme reddening for our two stars of $E(B - V) = 0.19$ (Schlegel, Finkbeiner, & Davis 1998), we would derive $\Delta[\text{Fe}/\text{H}] = +0.15$ with respect to the Pleiades. We adopt an error in the extinction of ± 0.02 so the error in our spectroscopic determination of $[\text{Fe}/\text{H}]$ rises to ± 0.08 . Nevertheless we caution the reader that this result has been derived from only two stars, and there is a great need to increase this sample. Unfortunately, most of the F stars have spectra which have large rotational broadening, so it may be necessary to pursue this work on the fainter G stars with larger telescopes.

Our new abundance is consistent with at least some other determinations of the abundance of NGC 2516. Twarog, Ashman, & Anthony-Twarog (1997) give $[\text{Fe}/\text{H}] = +0.060 \pm 0.030$ from DDO photometry of two stars. Nissen (1988) reports $uvby - \beta$ photometry of 6 stars in NGC 2516, deriving $[\text{Fe}/\text{H}] = +0.06 \pm 0.06$ and $E(b - y) = 0.081 \pm 0.016$, which corresponds to $E(B - V) = 0.11 \pm 0.02$. The Nissen et al. result, however, disagrees with that of Lyngå & Wramdemark (1984), who also report $uvby - \beta$ photometry in NGC 2516 and derive $[\text{Fe}/\text{H}] = -0.28$ using about the same extinction as Nissen (1988).

3.2. The distance and reddening to NGC 2516 and its photometric metallicity

We now present a new determination of the cluster distance and photometric metallicity using an updated version of the main-sequence fitting method outlined in Pinsonneault et

⁷For example, an alternative calibration of the color-temperature relation is provided by Houdashelt, Bell, & Sweigart (2000), who provide polynomial fitting functions in both $B - V$ and $V - I$. For the two stars in question, this temperature scale is 66 K cooler in $B - V$ than that from Saxner & Hammarbäck (1985) used in the abundance analysis. For the entire sample the mean difference is ≤ 25 K for any reddening $E(B - V) \leq 0.2$; it just so happens that our two stars with high S/N spectra have colors where the temperature difference between the two $B - V$ scales is a maximum.

al. (1998). The full details of the method may be found in Pinsonneault et al. (2002), and a preliminary determination for NGC 2516 is discussed in Pinsonneault, Terndrup & Yuan (2000).

The process of isochrone fitting separately in $B - V$ and $V - I$ yields a photometric metallicity for a cluster since the luminosity of the main sequence at fixed color changes more rapidly in $B - V$ (where $\Delta M_V / \Delta [\text{Fe}/\text{H}] \approx 1.3$) than it does in $V - I$ ($\Delta M_V / \Delta [\text{Fe}/\text{H}] \approx 0.6$). The signature of a metal poor cluster would then be a distance modulus derived in $B - V$ that was greater than found in $V - I$. Indeed, Jeffries, James & Thurston (1998) used this technique to derive $[\text{Fe}/\text{H}] = -0.18 \pm 0.05$ for NGC 2516, using the smaller sample of radial velocity members available then, while Pinsonneault, Terndrup & Yuan (2000) found $[\text{Fe}/\text{H}] = -0.26$ using the same data; both studies used $E(B - V) = 0.11$. As these are both at variance with our spectroscopic abundance (above), we wish to explore the distance and metallicity determinations in some detail.

Our approach here is similar in approach to that employed by Jeffries, Thurston, & Hambly (2001) in the determination of candidate photometric members of NGC 2516. In that study, they generated empirical isochrones starting with the Siess, Dufour, & Forestini (2000) models, and then calibrated the isochrones with multicolor photometry in the Pleiades, assuming a Pleiades distance modulus of 5.6. They derived a distance to NGC 2516 by fitting a 150 Myr isochrone to the main-sequence appearing in $B - V$ and $V - I$ CMDs, which is relatively distinct from the background except at faint magnitudes. The result of this calculation determined the relative distance between the Pleiades and NGC 2516. The result depended on the metallicity: for solar abundance, the distance is 8.10 ± 0.05 in both $B - V$ and $V - I$, while for half solar the distances in $B - V$ and $V - I$ were respectively 7.85 ± 0.05 and 7.90 ± 0.05 . Both calculations assumed $E(B - V) = 0.12$, and a particular choice of the extinction law. By comparison, the Hipparcos parallax translates to a distance modulus of $(m - M)_0 = 7.70 \pm 0.16$ (Robichon et al. 1999), which is close to the value of 7.77 ± 0.11 found by Sung et al. (2002). This last study presented $UBVI$ photometry for NGC 2516 independently of Jeffries, Thurston, & Hambly (2001), and derived a photometric metal abundance of $[\text{Fe}/\text{H}] = -0.10 \pm 0.04$ by comparison of the main sequence to uncalibrated isochrones from the Padua group. We will have more to say about the Sung et al. (2002) analysis below.

We begin the discussion by comparing the photometry of our radial velocity members to isochrones at the distance measured by Hipparcos. Figure 2 shows the color-magnitude diagram in V_0 and $(B - V)_0$ for the combined sample, where the filled points display photometry for our radial-velocity members and the open points show the Dachs & Kabus (1989) photometry for main-sequence members from the radial velocity study of González & La-

passet (2000). The stars deemed non-members from our radial velocities are displayed as plusses. Figure 3 displays a CMD in V_0 , $(V - I)_0$ for the magnitude range containing our sample only. The photometry has been dereddened according the prescription of Bessell, Castelli, & Plez (1998, their Appendix F) using a value $E(B - V)_0 = 0.12$ for hot stars and including the dependence of extinction and reddening on stellar color. In $B - V$, there is a tight single-star sequence with a distinctly brighter binary sequence; in $V - I$ there is no such clear separation and the main-sequence has a fairly wide range of colors. The dashed lines on Figures 2 and 3 show an isochrone for $[\text{Fe}/\text{H}] = 0.0$, calibrated as described below, and relocated to the Hipparcos distance. We conclude from Figures 2 and 3 that the Hipparcos distance and the similar Sung et al. (2002) value are correct only if NGC 2516 is metal poor (about $[\text{Fe}/\text{H}] = -0.3$), provided that the distance modulus to the Pleiades is near 5.6. Alternatively, NGC 2516 may share the Pleiades “problem” (Pinsonneault et al. 1998) of having a Hipparcos parallax that makes the cluster considerably fainter than expected for its metal abundance as derived in this paper.

The isochrones were derived from evolutionary tracks incorporating angular momentum transport and an updated equation of state (Sills, Pinsonneault, & Terndrup 2000; Tinker, Pinsonneault, & Terndrup 2002). The tracks are first used to generate isochrones in the theoretical plane (i.e., M_V , T_{eff}). An initial calibration to $BVRI$ colors comes from the Lejeune, Cuisinier, & Buser (1997) model atmospheres. The colors are then further corrected to match the photometry of single star members of the Hyades⁸ cluster; this step is necessary because the isochrone shapes after initial calibration still do not match the observed cluster main sequence at all luminosities (e.g., Terndrup et al. 2000, their Figs. 4 and 5). Parallaxes for individual Hyades members, which have typical errors of 2%, were used to correct the photometry to the distance of the dynamical center of the cluster which has a distance modulus 3.34 ± 0.01 , or $d = 46.6 \pm 0.2$ pc (Perryman et al. 1998). The empirical corrections were generated for a theoretical isochrone with $[\text{Fe}/\text{H}] = +0.13$ (Boesgaard & Friel 1990), with scaled solar abundances and the solar helium abundance. The empirical color corrections can then be applied to isochrones of any age and metallicity. For metallicities within a few tenths dex of solar the empirical corrections to the colors are assumed to be independent of metallicity; this is equivalent to assuming that the effect of line blanketing on the colors is correct in the model atmospheres employed in the initial calibration of the isochrones.

In the Pinsonneault et al. (2002) method, cluster distances are then found by determin-

⁸In its full detail, the Pinsonneault et al. (2002) method also includes fainter Pleiades stars to extend the empirical calibration to redder colors than are available for Hyades stars with Hipparcos parallaxes; this consideration does not, however, make a difference here to NGC 2516 since our survey only extends to about $(B - V)_0 = 0.9$, a color range completely spanned by Hyades stars with excellent Hipparcos parallaxes.

ing $V_0 - M_V$ for each star, where M_V is the absolute magnitude of the empirically calibrated isochrone at the dereddened color of the star, and V_0 is the dereddened magnitude. The cluster distance is found separately in $B - V$ and $V - I$ from the median value of $V - M_V$ in color bins. Stars that are more than 0.1 mag from the median are rejected, which reduces the effect of binaries on the distance determination. The distance modulus is derived for isochrones of several different metallicities. The cluster photometric metallicity is taken as the metallicity of the isochrone for which the distance moduli determined from $B - V$ and $V - I$ agree. In addition, it is generally possible to use the narrowness of the main sequence in $B - V$ as a measure of whether the shape of a particular isochrone matches the main sequence data in that color; a shape mismatch is indicated by finding that $\langle V_0 - M_V \rangle$ is a function of color.

There are two problems which arise in determining the distance and photometric metallicity of NGC 2516. First, the cluster has a markedly higher reddening than most of the clusters in the original study of Pinsonneault et al. (1998). The derived photometric metallicity depends sensitively on the adopted reddening value, the ratio of total to selective extinction in the various photometric bands, and whether there is differential reddening towards the cluster. Second, the large span in color of the main sequence in $V - I$ (Fig. 3) means that there will be a wide range of statistically permitted values of the apparent distance modulus in the $(V, V - I)$ CMD; as a consequence, the photometric metallicity will have a relatively large error compared to clusters with narrow sequences. The width of the main sequence in $V - I$ may be caused by a significant binary fraction in the cluster, any observational selection favoring binaries over single stars, or by significant differential extinction towards NGC 2516.

Previous studies of the extinction towards NGC 2516 have generally arrived at values near $E(B - V) = 0.11$ or 0.12 (Dachs & Kabus 1989; Sung et al. 2002, and references therein). In contrast, the Schlegel, Finkbeiner, & Davis (1998) dust-emission maps in the direction of NGC 2516 indicate a higher average reddening $\langle E(B - V) \rangle = 0.21$ to our spectroscopic members, with a variation of $\Delta E(B - V) = 0.03$ towards our target stars. That the average reddening is higher than that obtained from the hot turnoff stars in the cluster is not, perhaps, a surprise, since the maps are based on the integrated infrared emission out to infinity and the cluster is located at a distance of about 400 pc at a galactic latitude of $b = -16^\circ$. Also, some studies (Arce & Goodman 1999; von Braun & Mateo 2001) have claimed that the Schlegel, Finkbeiner, & Davis (1998) maps overestimate the extinction by 30–50% when $A_V > 0.5$ (equivalently when $E(B - V) \geq 0.15$).

In this analysis, we attempted to fit isochrones of a wide variety of metallicities using the sample of radial velocity members in Table 1, and allowed the reddening to vary from the

previously determined values. Low metallicities ($[\text{Fe}/\text{H}] \leq -0.4$) provided a poor fit to the isochrone shapes at any value of the reddening. Statistically acceptable fits were obtained for metallicities between $[\text{Fe}/\text{H}] = -0.3$ and $+0.1$ at reddenings between $E(B - V) = 0.12$ and 0.18 . For the canonical reddening of $E(B - V) = 0.12$, the photometric metallicity for NGC 2516 is $[\text{Fe}/\text{H}] = -0.05$ at a distance of $V_0 - M_V = 7.93$. We illustrate this solution in Figures 2 and 3, where the best fitting isochrone is displayed as a solid lines in each figure. In $B - V$, this isochrone runs through the single-star sequence, and runs along the lower edge of the main sequence in $V - I$. The match of the isochrone shapes to the photometry is shown in Figure 4, which shows the individual values in $V_0 - M_V$ in each color. There is no significant trend with magnitude in the residuals in either color.

We extensively explored the sensitivity of the determination of the distance and photometric metallicity to choices of reddening and the reddening law. The results are summarized in Table 3. The smallest source of error is the accuracy of finding the median apparent distance modulus. The largest source of error is the value of the extinction itself. Adopting higher extinctions increases the photometric metallicity appreciably but reduces the derived distance only slightly; the effect on the distance modulus is smaller since the slope of reddening vector is only somewhat different from the average slope of the main sequence. An equally important source of error is the steepness of the adopted extinction law, which may be characterized by the value of $R_{\text{VI}} \equiv E(V - I)/E(B - V)$. Increasing R_{VI} results in a smaller distance and a significantly higher photometric metallicity. The final values we derive for NGC 2516 are $[\text{Fe}/\text{H}] = -0.05 \pm 0.14$ and $V_0 - M_V = 7.93 \mp 0.14$.

Adopting an $E(B - V)$ error of ± 0.02 , then the photometric metallicity we found for NGC 2516 is consistent, within the errors, with the value of $+0.01 \pm 0.08$ we find from our spectroscopic analysis. The main reason we derive a higher metallicity from the CMD here than did Pinsonneault, Terndrup & Yuan (2000) is because we employ the Bessell, Castelli, & Plez (1998) extinction law, for which $R_{\text{VI}} = 1.34$ at the mean $V - I$ of our sample, in contrast to the value $R_{\text{VI}} = 1.25$ used in the previous determinations of the metallicity from the CMD. In our analysis, we took ± 0.04 for the error in R_{VI} , representing the difference between the adopted value and the Dean, Warren, & Cousins (1978) value of $R_{\text{VI}} = 1.30$ for the average color in our sample. The reddening law we used here has $A(V)/E(V - I) = 2.47$, on average, which is equal to the value of 2.49 ± 0.02 determined empirically from observations of stars in the bulge by Stanek (1996).

The distance we determine is 1.5σ higher than the Hipparcos value, which is not a statistically significant difference by itself. This difference corresponds to a difference in parallax of 0.29 mas, quite a bit smaller than the $1 - 2$ mas systematic errors in the parallaxes needed to explain the difference between the Hipparcos and isochrone-fitting distance to the

Pleiades (Pinsonneault et al. 1998; Narayanan & Gould 1999). Reconciling the photometric distance with the Hipparcos distance would require the photometric metallicity to be lower than we determine, which would make that metallicity inconsistent with our spectroscopic value.

If instead we adopted our spectroscopic value and fit a solar abundance isochrone to the narrow $B - V$ sequence in Figure 2, we would obtain a more precise distance of $(V_0 - M_V) = 8.05 \pm 0.11$, which is 2.5σ higher than the Hipparcos distance.

Recently, Sung et al. (2002) analyzed new $UBVI$ photometry of NGC 2516, and used the Padua group isochrones to derive a photometric metallicity of $[\text{Fe}/\text{H}] = -0.10 \pm 0.04$ and a distance modulus $V_0 - M_V = 7.77 \pm 0.11$. Therefore despite finding a relatively high abundance for NGC 2516, their distance is consistent with the Hipparcos value. In our opinion, their analysis is seriously flawed, even though their distance determination is marginally equal to ours within the errors. Here we have demonstrated that one can achieve an excellent fit to the CMD in both $B - V$ and $V - I$ from isochrones calibrated on the Hyades and the Pleiades. An inspection of Figure 2 in Sung et al. (2002) shows that the isochrones they adopted do not simultaneously fit the main sequences in $B - V$ and $V - I$ and are a poor match to the shape of the main sequence in $B - V$ or $U - B$. Their determination of the distance rests primarily on fitting an isochrone to the $(V, V - I)$ CMD; the corresponding isochrone in $B - V$ is significantly too bright (or red) and misses the bulk of the main sequence over at least 5 mag in V . They then attribute the difference between the isochrone and the stellar locus to a UV excess, and claim that this is a general feature of young stellar clusters. Finally, they determine the cluster metallicity by rejecting most of the stars in the cluster as having a UV excess, which necessarily means that they derived a value near solar because their sample is contaminated with nonmembers. In a separate paper (Stauffer et al. 2002), we present evidence for a blue excess in young, low-mass stars, mainly from data for late-K dwarfs in the Pleiades. We find no evidence for blue excesses in G and early K dwarfs, and hence we do not believe that this phenomenon should affect the results we have presented for NGC 2516.

3.3. Other metallicity estimates

Debernardi & North (2001) have recently published a detailed study of the eclipsing binary system V392 Car, which is a member of NGC 2516. They compared their derived luminosity for the members of this system against stellar structure models using a distance close to the Hipparcos measurement, and derived a metallicity of $[\text{Fe}/\text{H}] = 0.0 \pm 0.1$. We performed a similar analysis, instead comparing the stars' measured radii to that in the

isochrones we used for the distance analysis. The result is $[\text{Fe}/\text{H}] = -0.05 \pm 0.05$ for these stars by the constraint that their radii match the isochrone radii, consistent within the errors with our spectroscopic determination.

4. Stellar rotation in NGC 2516

Following the approach of Soderblom, Jones, & Fischer (2001) and Soderblom et al. (1993), we display in Figure 5 the correlation between $v \sin i$ and color for NGC 2516 and other well-studied open clusters. From top to bottom are shown the Pleiades, NGC 2516, M 34 and the Hyades (600 Myr). The data sources are as follows: Pleiades: Queloz et al. (1999), supplemented with new observations in Terndrup et al. (2000); NGC 2516: this paper; M 34: Soderblom, Jones, & Fischer (2001); Hyades: $v \sin i$ data from Kraft (1965, 1967), and rotational periods from Radick et al. (1987) converted to $v \sin i$. The solid line in each panel is a representation of the Hyades data, while the dashed line indicates the location of the rapid rotators in the Pleiades. For NGC 2516, we adopted $E(B - V) = 0.12$ (above).

In Fig. 5, the time evolution of angular momentum from the Pleiades to the Hyades (100 to 600 Myr) manifests itself as a gradual reduction in $v \sin i$ for the slow rotators, and a significant decline in the numbers of rapid rotators. NGC 2516, like the Pleiades, has a number of rapid rotators, and these have rotation speeds about 70% of the stars in the Pleiades with similar colors. The number of rapid rotators declines markedly by the age of M 34, which has an age estimated from 180 Myr (Meynet, Mermilliod, & Maeder 1993) to ~ 250 Myr (Jones & Prosser 1996). In M 34, the upper bound of rotation rates is about a factor of two lower than it is in the Pleiades. Our observations in NGC 2516 do not extend to the faint magnitudes at which the K dwarfs in the Pleiades and M 34 are still rapidly rotating.

In Figure 6, we compare the rotation rates of stars in the Pleiades, NGC 2516, M 34 and the Hyades with theoretical models. The data sources are the same as in Figure 5. The conversion between color and effective temperature is taken from Houdashelt, Bell, & Sweigart (2000). The models are taken from Sills, Pinsonneault, & Terndrup (2000), and are for solar metallicity stars. The adopted ages of the clusters are shown in figure 6, where we have taken the Jones & Prosser (1996) age of 250 Myr for M 34 as in their paper. In the models the stars are assumed to be differentially rotating. The loss of angular momentum from the surface was modelled using a saturated magnetic wind loss law (Chaboyer, Demarque, & Pinsonneault 1995) with a mass-dependent saturation threshold ω_{crit} which follows a Rossby scaling down to $M = 0.5M_{\odot}$ and then chosen to match the low mass rapid rotators

in the Hyades. We used five different values of the disk-locking lifetime, during which the star is assumed to be rotating at the same rate as its proto-stellar disk. The lifetimes are chosen to span the expected range of proto-stellar disk lifetimes, up to 10 Myr.

The overall impression from Figure 6 is that the rotation rates of the stars in NGC 2516 are similar to what would be expected at an age near 140 Myr if the angular momentum evolution of intermediate mass stars ($M = 0.6 - 1.1M_{\odot}$) in all clusters was similar. In this plot, M 34 has a few stars with rotation rates significantly higher than the fastest-spinning model. This may represent a departure from the suggested uniformity of the Pleiades : NGC 2516 : Hyades evolution, or else the age of M 34 is closer to the value of 180 Myr from Meynet, Mermilliod, & Maeder (1993) than the 250 Myr shown here. Establishing that different star clusters represent time snapshots of a universal evolution of angular momentum thus would require better age estimates for these clusters than is currently available.

The data for both NGC 2516 and M 34 probe only the intermediate mass stars, and do not extend to the low mass stars where the standard Rossby scaling breaks down. There is a substantial change in behavior of the low mass models in this age range depending on the choice of the saturation threshold (standard Rossby scaling vs. the Sills, Pinsonneault, & Terndrup (2000) fit to the Hyades data).

If initial conditions for star formation were universal, we would expect that the distribution of disk lifetimes would be the same from cluster to cluster, and should not depend on the age of the cluster. It appears that the Pleiades and NGC 2516 have similar fractions of stars with disk lifetimes between 0 and 1 Myr. However, the expected rotation rates for stars with disk lifetimes longer than 1 Myr are slow enough that they overlap with our observational limits. We cannot say whether the distribution is the same without better resolution of rotation rates or photometric period determinations.

In Figure 7 we plot the fractional luminosity in X-rays ($L_{\text{X}}/L_{\text{bol}}$) for NGC 2516 against the inverse of Rossby number, which is defined as the ratio of the rotation period to the turnover of time of a convective cell at the base of the convective zone. The X-ray luminosities were taken from Jeffries, Thurston, & Pye (1997); filled points show measured values, while filled triangles show upper limits on the X-ray detection. The open points show equivalent data for a set of Pleiades stars with known rotation periods (Krishnamurthi et al. 1998). In order to treat both data sets the same way, we ignored the rotation periods for the Pleiades stars and instead began with $v \sin i$ values for these. The measured values for $v \sin i$ were used to compute a rotation period using the empirically calibrated isochrones employed above, and the isochrones were used to generate relations between effective temperature and the $B - V$ and $V - I$ colors. The convective overturn time was computed from the effective temperature using the prescription in Kim & Demarque (1996). We did not apply

a statistical correction for projection to the data, which would have increased the $v \sin i$ values by a factor of $4/\pi = 1.27$. The conclusion from Figure 7 is that both the Pleiades and NGC 2516 have the same relation between convection zone depth and X-ray activity. The Pleiades stars plotted here have a higher average rotation rate and X-ray luminosity, but the (fewer) rapid rotators in NGC 2516 are similar. The bulk of the NGC 2516 data lie amongst the more slowly-rotating Pleiades; again there is no obvious difference between the two clusters.

5. Summary and discussion

The principal result of this paper is the demonstration that NGC 2516 has approximately solar metallicity, which we showed from an equivalent width analysis on high signal-to-noise spectra and from the location of the main sequence on CMDs. While the metallicity from the latter method has rather large errors, both random and systematic, it is nevertheless consistent with the metallicity found from our spectra. We also showed that the rotational and X-ray properties of the F and early G stars in NGC 2516 are consistent with what would be expected at an age near 140 Myr if angular momentum evolution in different clusters is a uniform time sequence.

Why, then, did previous studies come up with values of the metallicity that were almost always metal poor? Both Cameron (1985) and Jeffries, Thurston, & Pye (1997) concluded the cluster was metal poor by modeling the colors in the $U - B$, $B - V$ plane, where the data were a combination of photographic and photoelectric photometry. The F stars in NGC 2516 clearly showed an ultraviolet excess compared to similar stars in the Pleiades (Jeffries, Thurston, & Pye (1997), their Figs. 10 and 11). The new CCD photometry that we report here from Jeffries, Thurston, & Hambly (2001) compares quite favorably to the previous values in $B - V$ over the magnitudes of stars in our sample, though the new study does not include photometry in U for an independent check of the zero point in that band.

On the other hand, our conclusion that NGC 2516 has approximately solar metallicity helps explain many other observations of the cluster. For example, Micela et al. (2000) analyzed Rosat HRI observations of NGC 2516 stars, and showed that the X-ray activity in this cluster is consistent with that observed in dK and dM stars of similar age, contrary to the expectation that the convection properties in NGC 2516 stars would be different than in solar-metallicity clusters. The depletion patterns of Li in this cluster are consistent with a metallicity near solar (Jeffries, James & Thurston 1998), but would require nonstandard mixing scenarios if the cluster were metal poor.

Extending our work to lower masses where rapid rotation is observed (e.g., Figure 5) is clearly warranted. Since NGC 2516 is significantly more distant than the Pleiades, $v \sin i$ studies amongst the M dwarfs would require telescopes in the 8-10m range (M dwarfs have $V \geq 14$ in the Pleiades, or $V > 16.6$ in NGC 2516).

We would like to thank the directors and staff of both CTIO and the Anglo-Australian Observatory. AF was a Particle Physics and Astronomy Research Council (PPARC) research student during this work. DMT and MHP acknowledge partial support from the National Science Foundation, via grants AST-9528227 and AST-9731621 to The Ohio State University.

REFERENCES

Arce, H., & Goodman, A. 1999, ApJ, 512, L135

Allain, S. 1998, A&A, 333, 629

Attridge, J. M., & Herbst, W. 1992, ApJ, 398, L61

Barrado y Navascués, D., Stauffer, J. R., & Patten B. M. 1999, ApJ, 522, 53

Bessell, M. S., Castelli, F., & Plez, B. 1998, A&A, 337, 321

Boesgaard, A. M., Budge, K., & Burck, E. E. 1988, ApJ, 325, 749

Boesgaard, A. M., Budge, K., & Ramsay, M. E. 1988, ApJ, 327, 389

Boesgaard, A. M., & Friel, E. D. 1990, ApJ, 351, 467

Cameron, A. C., & Campbell, C. G. 1993, A&A, 274, 309

Cameron, L. M. 1985, A&A, 147, 39

Chaboyer, B., Demarque, P., & Pinsonneault, M. H. 1995, ApJ, 441, 865

Crawford, D., & Perry, C. 1976, AJ, 81, 419

Dachs, J., & Kabus, H. 1989, A&AS, 78, 25

Dean, J. F., Warren, P. R., & Cousins, A. W. J. 1978, MNRAS, 183, 569

Debernardi, Y. & North, P. 2001, A&A, 374, 204

Eggen, O. J. 1972, ApJ, 173, 63

González, J. F., & Lapasset, E. 2000, AJ, 119, 2296

Gray, D. F. 1992, The Observation and Analysis of Stellar Photospheres, 2nd edition, Cambridge University Press, Cambridge

Harnden, F. R., et al. 2001, ApJ, 547, L141

Hartmann, L., Hewett, R., Stahler, S., & Mathieu, R. 1986, ApJ, 309, 275

Herbst, W., Bailer-Jones, C. A. L., & Mundt, R. 2001, ApJ, 554, L197

Herbst, W., Rhode, K. L., Hillenbrand, L. A., & Curran, G. 2000, AJ, 119, 261

Houdashelt, M. L., Bell, R. A., & Sweigart, A. V. 2000, AJ, 119, 1448

James, D. J., & Jeffries, R. D. 1997, MNRAS, 292, 252

Jeffries, R. D. 1997, MNRAS, 288, 585

Jeffries, R. D., James, D. J., & Thurston, M. R. 1998, MNRAS, 300, 550

Jeffries, R. D., Thurston, M. R., & Hambly, N. C. 2001, A&A, 375, 863

Jeffries, R. D., Thurston, M. R., & Pye, J. P. 1997, MNRAS, 287, 350

Jones, B. F., Fischer, D. A., & Stauffer, J. R. 1996, AJ, 112, 1562

Jones, B. F., Fischer, D., Shetrone, M., & Soderblom, D. R. 1997, AJ, 114, 352

Jones, B. F., & Prosser, C. F. 1996, AJ, 111, 1193

Kawaler, S. D. 1998, ApJ, 333, 236

Keppens, R., MacGregor, K. B., & Charbonneau, P. 1995, A&A, 294, 469

Kim, Y.-C., & Demarque, P. 1996, ApJ, 457, 340

Koester, D. & Reimers, D. 1996, A&A, 313, 810

Königl, A. 1991, ApJ, 370, L39

Kraft, R. P. 1965, ApJ, 142, 681

Kraft, R. P. 1967, ApJ, 150, 551

Krishnamurthi, A., et al. 1998, ApJ, 493, 914

Krishnamurthi, A., Pinsonneault, M. H., Barnes, S., & Sofia, S. 1997, *ApJ*, 475, 604

Kurucz, R. L. 1993, Kurucz CD-Rom 13, *Atlas* 9, SAO, Cambridge

Landolt, A. U. 1992, *AJ*, 104, 340

Lejeune, Th., Cuisinier, F., & Buser, R. 1997, *A&AS*, 125, 229

Lyngå, G. 1987, Technical Report, Catalogue of Open Cluster Data., 5th ed., Lund Observatory

Lyngå, G., & Wramdemark, S. 1984, *A&A*, 132, 58

MacGregor, K. B., & Brennan, M. 1991, *ApJ*, 376, 204

Meynet, G., Mermilliod, J.-C., & Maeder, A. 1993, *A&AS*, 98, 477

Micela, G., Sciortino, S., Jeffries, R. D., Thurston, M. R., & Favata, F. 2000, *A&A*, 357, 909

Milford, P. N., O'Mara, B. J., & Ross, J. E. 1994, *A&A*, 292, 276

Mills, D., Webb, J., & Clayton, M. 1997, Starlink User Note 152.4, Rutherford-Appleton Laboratories

Narayanan, V. K., & Gould, A. 1999, *ApJ*, 523, 328

Nissen, P. E. 1988, *A&A*, 199, 146

Perryman, M. A. C., Brown, A. G. A., Lebreton, Y., Gomez, A., Turon, C., de Strobel, G. C., Mermilliod, J.-C., Robichon, N., Kovalevsky, J., & Crifo, F. 1998, *A&A*, 331, 81

Pinsonneault, M. H., DePoy, D. L., & Coffee, M. 2001, *ApJ*, 556, 59

Pinsonneault, M. H., Stauffer, J., Soderblom, D. R., King, J. R., & Hanson, R. B. 1998, *ApJ*, 504, 170

Pinsonneault, M. H., Terndrup, D. M., Stauffer, J. R., & Hanson, R. B. 2002, in preparation

Pinsonneault, M. H., Terndrup, D. M., & Yuan, Y. 2000, in Stellar Clusters and Associations: Convection, Rotation, and Dynamics, ed. R. Pallavicini, G. Micela, & S. Sciortino, *ASP Conf. Ser.* 198, 95

Queloz, D., Allain, S., Mermilliod, J.-C., Bouvier, J., & Mayor, M. 1998, *A&A*, 335, 183

Radick, R. R., Thompson, D. T., Lockwood, G. T., Duncan, D. K., & Baggett, W. E. 1987, *ApJ*, 321, 459

Rebull, L. M. 2001, AJ, 121, 1676

Robichon, N., Arenou, F., Mermilliod, J.-C., & Turon, C. 1999, A&A, 345, 471

Saxner, M., & Hammarbäck, G. 1985, A&A, 151, 372

Schatzman, E. 1962, Ann. d'Ap., 25, 18

Schlegel, D. J., Finkbeiner, D. P., & Davis, M. 1998, ApJ, 500, 525

Sciortino, S., et al. 2001, A&A, 365, L259

Seiss, L., Dufour, E., & Forestini, M. 2000, A&A, 358, 593

Shu, F. H., Najita, J., Ruden, S. P., & Lizano, S. 1994, ApJ, 429, 797

Sills, A., Pinsonneault, M. H., & Terndrup, D. M. 2000, ApJ, 534, 335

Smith, K. C. 1992, PhD thesis, University of London

Soderblom, D. R., Jones, B. F., & Fischer, D. 2001, ApJ, 563, 334

Soderblom, D. R., Stauffer, J. R., Hudon, J. D., & Jones, B. F. 1993, ApJS, 83, 315

Stanek, K. Z. 1996, ApJ, 460, L37

Stassun, K. G., Mathieu, R. D., Mazeh, T., & Vrba, F. J. 1999, AJ, 117, 2941

Stauffer, J. R., et al. 1999, ApJ, 527, 219

Stauffer, J. R., Balachandran, S., Krishnamurthi, A., Pinsonneault, M. H., Terndrup, D. M., & Stern, R. A. 1997, ApJ, 475, 604

Stauffer, J. R., & Hartmann, L. 1987, ApJ, 318, 337

Stauffer, J. R., Hartmann, L. W., & Jones, B. F. 1989, ApJ, 346, 160

Stauffer, J. R., Hartmann, L. W., & Latham, D. W. 1987, ApJ, 320, L51

Stauffer, J. R., Jones, B. F., Backman, D., Pinsonneault, M., Hartmann, L. W., Barrado y Navascués, D., & Terndrup, D. M. 2002, in preparation

Stauffer, J. R., Shultz, G., & Kirkpatrick, J. D. 1998, ApJ, 499, 199

Stover, R. J. 1998, in Instrumentation for Ground-Based Optical Astronomy, Present and Future, ed. L. B. Robinson, (New York: Springer-Verlag), 443

Stefanik, R. P., Latham, D. W., & Torres, G. 1999, in Precise Stellar Radial Velocities, IAU Colloquium 170, eds. J. B. Hearnshaw & C. D. Scarfe, ASP Conf. Ser. 185, 345

Sung, H., Bessell, M. S., Lee, B.-W., & Lee, S.-G. 2002, AJ, 123, 290

Terndrup, D. M., Stauffer, J. R., Pinsonneault, M. H., Sills, A., Yuan, Y., Jones, B. F., Fischer, D., & Krishnamurthi, A. 2000, AJ, 119, 1303

Tinker, J., Pinsonneault, M. H., & Terndrup, D. M. 2002, ApJ, 564, 877

Twarog, B. A., Ashman, K. M., & Anthony-Twarog, B. J. 1997, AJ, 114, 2556

Udry, S., Mayor, M., & Queloz, D. 1999, in Precise Stellar Radial Velocities, IAU Colloquium 170, eds. J. B. Hearnshaw & C. D. Scarfe, ASP Conf. Ser. 185, 367

von Braun, K., & Mateo, M. 2001, AJ, 121, 1522

von Hippel, T., & Gilmore, G. 2000, AJ, 120, 1384

Weber, E. J., & Davis, L. 1967, ApJ, 148, 217

Weidemann, V. 2000, A&A, 363, 647

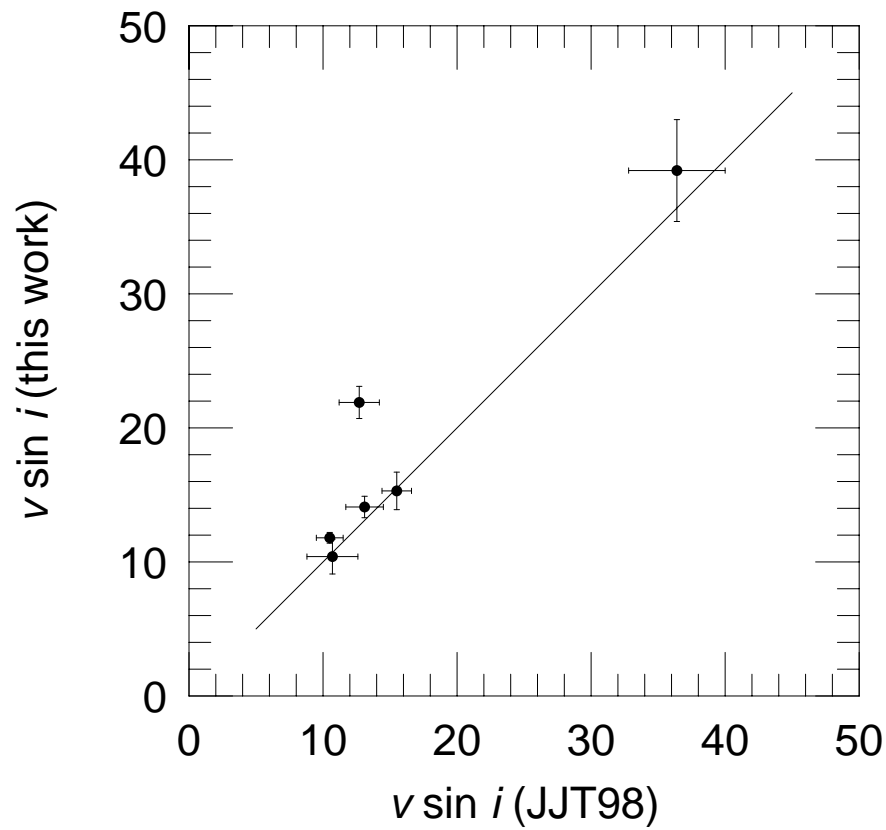


Fig. 1.— Comparison of new and previously published values of $v \sin i$. The ordinate displays $v \sin i$ values from this work, while the abscissa shows those measured by Jeffries et al. (1998). The 1σ error bars are also shown. The discrepant point is for the star DK 206, discussed in the text.

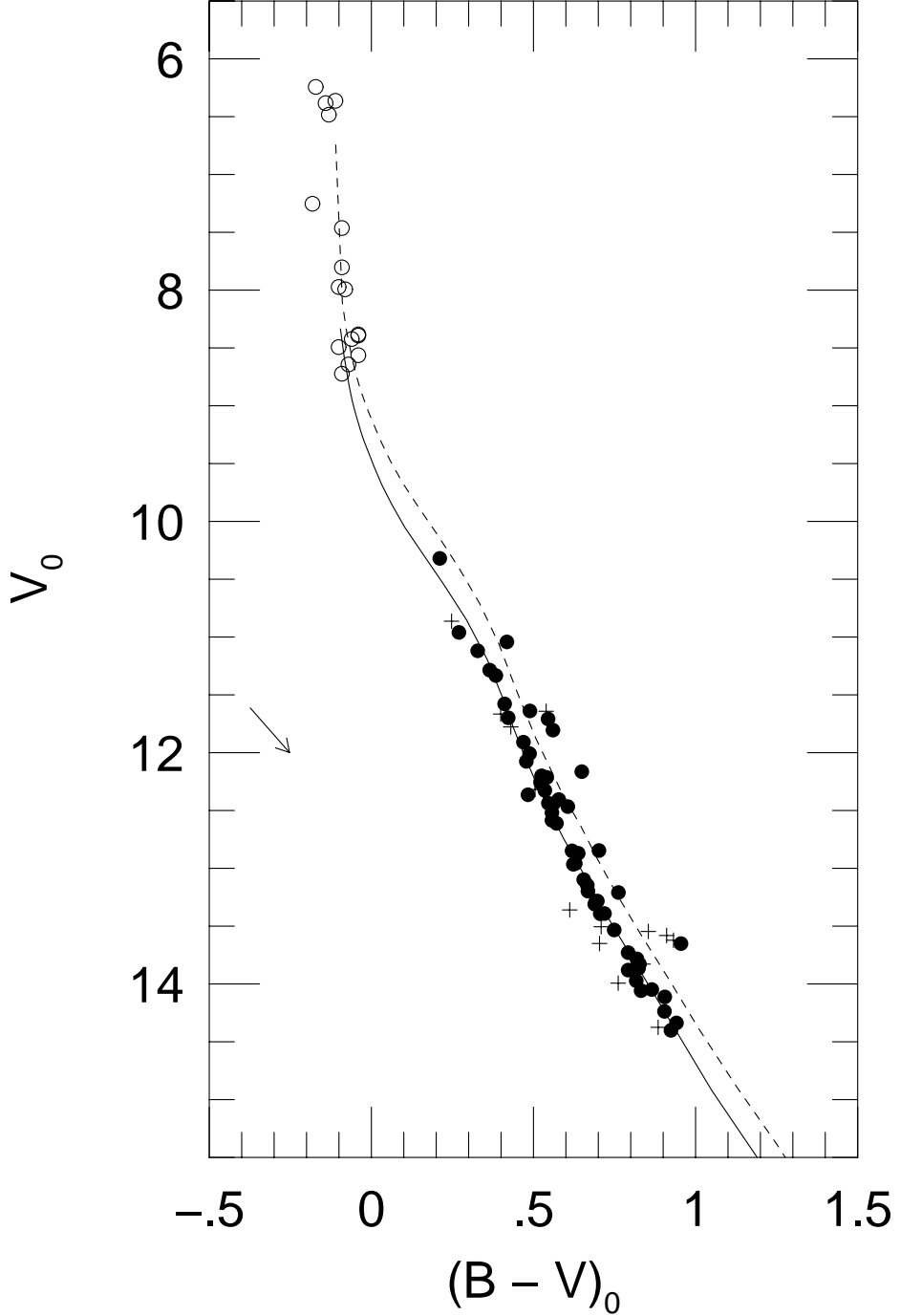


Fig. 2.— Color-magnitude diagram in V , $B - V$ for NGC 2516. Filled points are for radial velocity members from this survey, while the open points are for bright members in the study of González & Lapasset (2000). Plus signs denote non-members from this paper. The photometry has been dereddened using $E_0(B - V) = 0.12$ and the extinction law derived by Bessell, Castelli, & Plez (1998). The dashed line shows a 140 Myr isochrone, empirically calibrated as described in the text, shifted to $V_0 - M_V = 7.70$, the Hipparcos distance to NGC 2516 (Robichon et al. 1999). The solid line shows the solution from this paper, namely $(V_0 - M_V) = 7.93$ and $[\text{Fe}/\text{H}] = -0.05$. The arrow denotes the reddening vector.

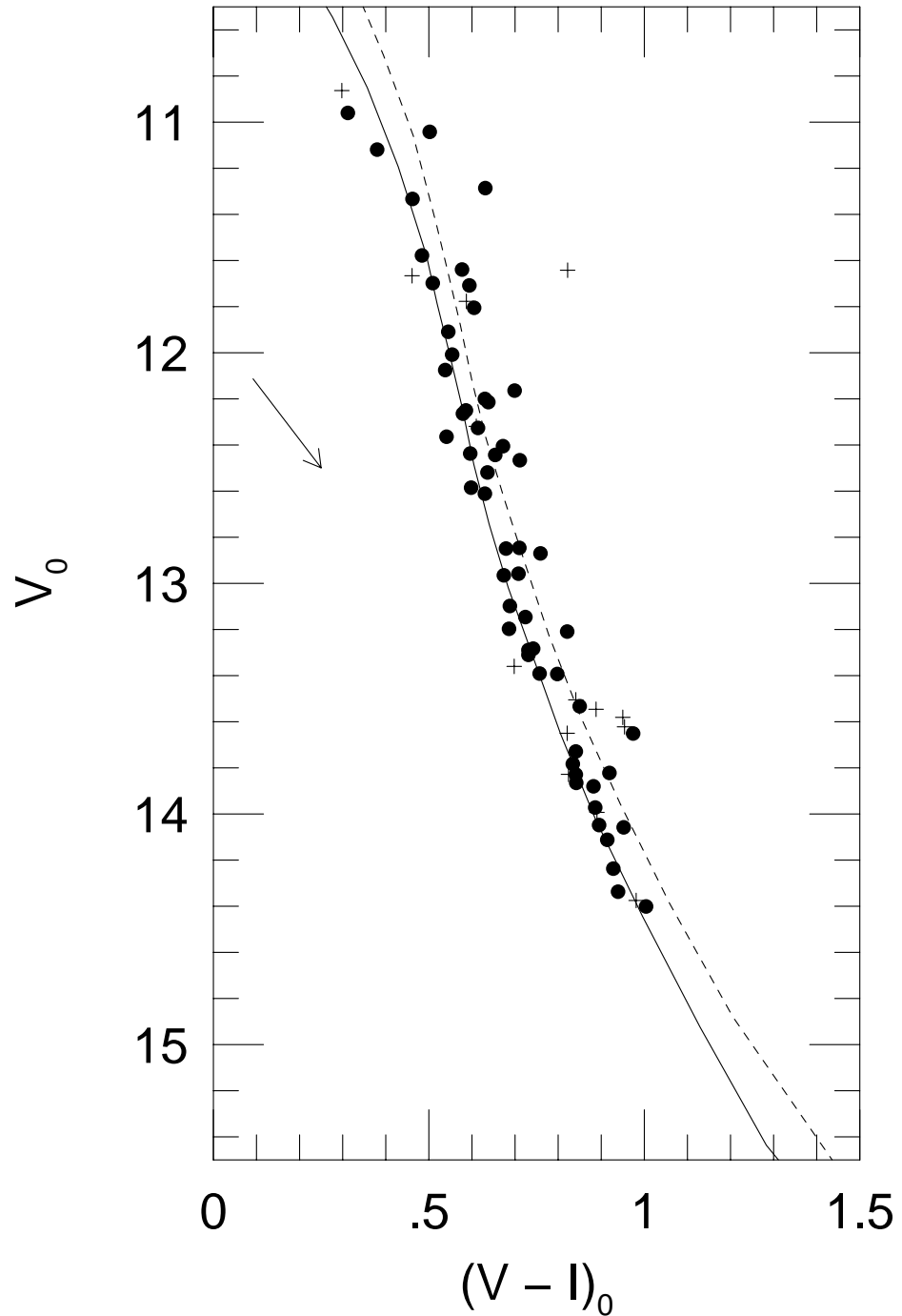


Fig. 3.— Color-magnitude diagram in V , $V - I$ for NGC 2516. Symbols and isochrones are the same as in Fig. 2. Note the change in scale with respect to Fig. 2.

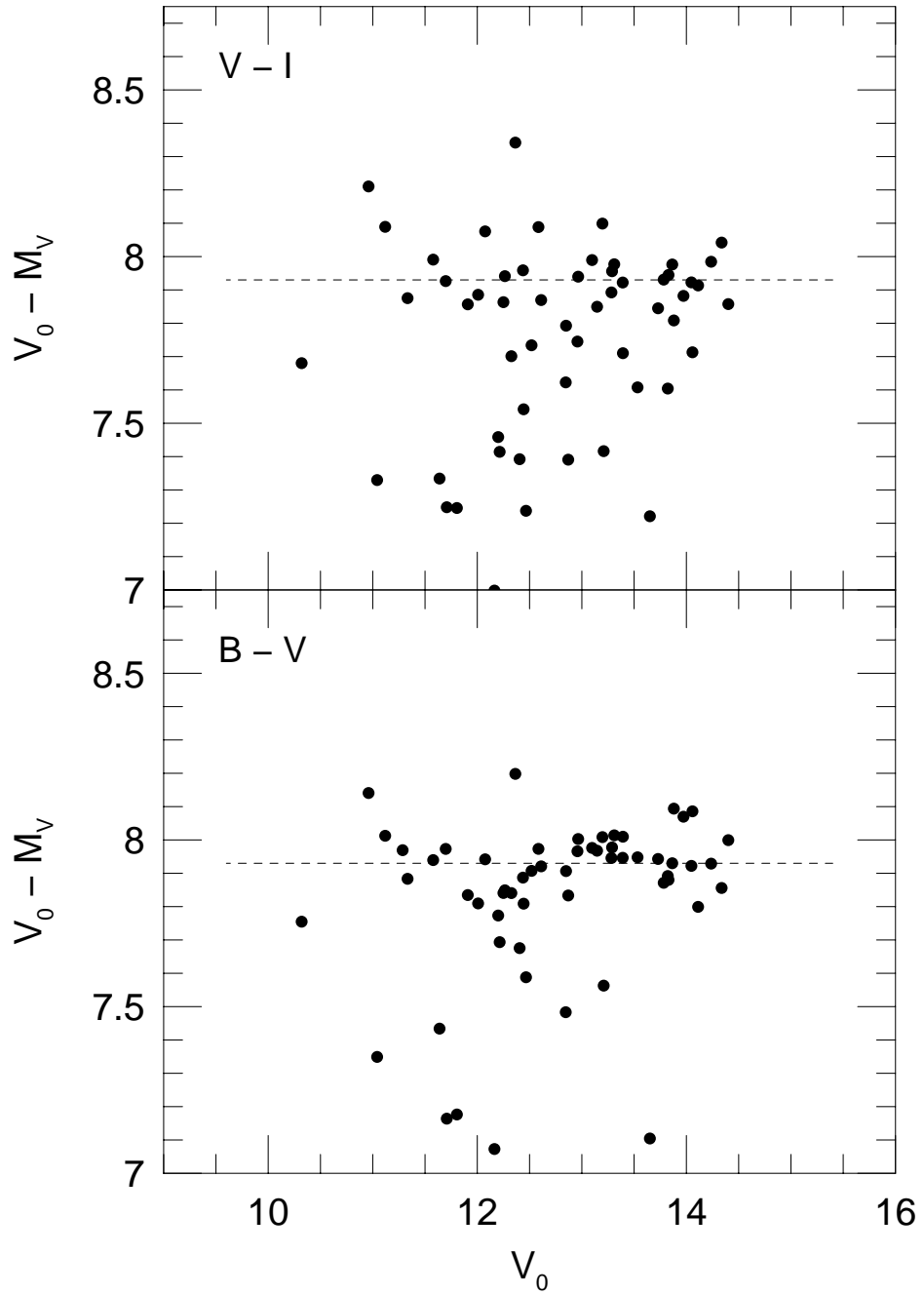


Fig. 4.— Differences between the dereddened V magnitude and an empirically calibrated isochrone for $[\text{Fe}/\text{H}] = -0.05$. The top panel shows the differences with respect to the isochrone in $V - I$, while the lower panel shows these in $B - V$. The dashed line shows the best fitting distance modulus $V_0 - M_V = 7.93$.

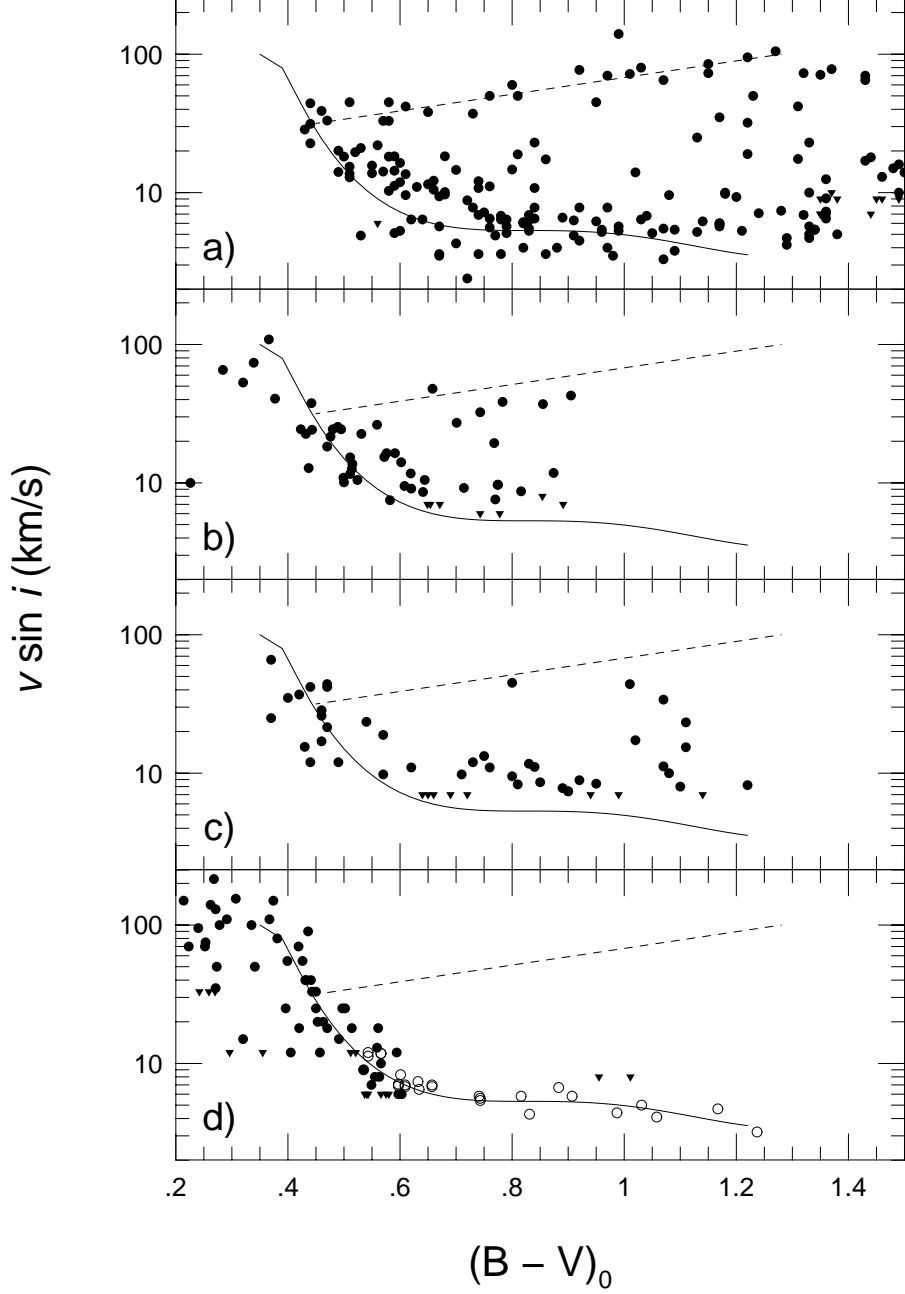


Fig. 5.— Comparison of $v \sin i$ for (a) Pleiades, (b) NGC 2516, (c) M 34, (d) Hyades. Sources for the rotation rates are described in the text. The solid line represents the mean Hyades relation, while the dashed line characterizes the fast rotators in the Pleiades; these lines are the same in all panels. Filled points denote measured $v \sin i$ values, while open points show $v \sin i$ derived from photometric rotation periods. Upper limits to $v \sin i$ are displayed as triangles.

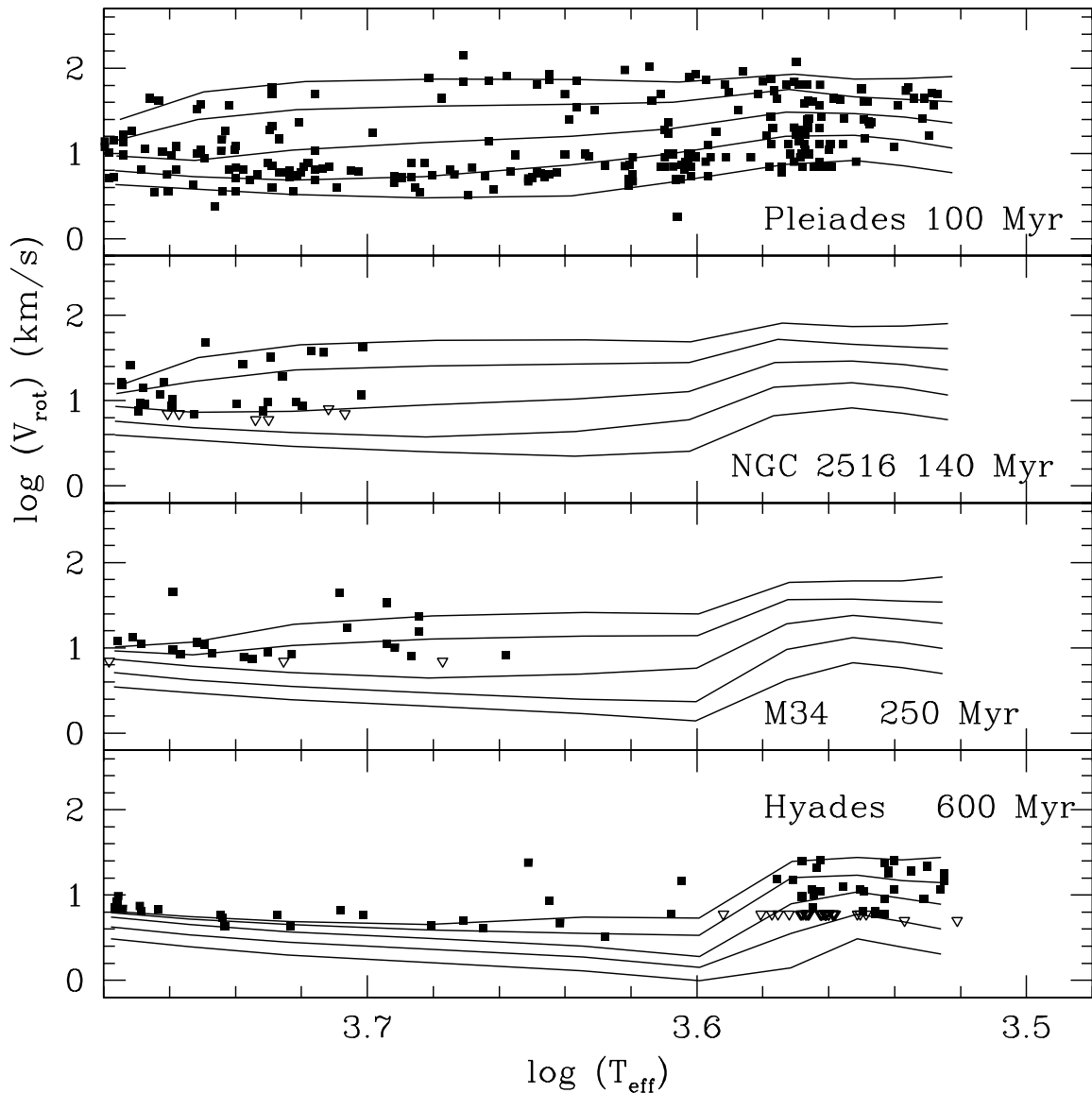


Fig. 6.— Rotation rate as a function of effective temperature for stars in young open clusters with ages between 100 Myr and 600 Myr. The assumed ages of the clusters are shown in each figure. The solid points are detections and the open triangles are upper limits. The solid lines show the five different values of the disk-locking lifetime that were used: 0, 0.3, 1, 3, and 10 Myr (from top to bottom).

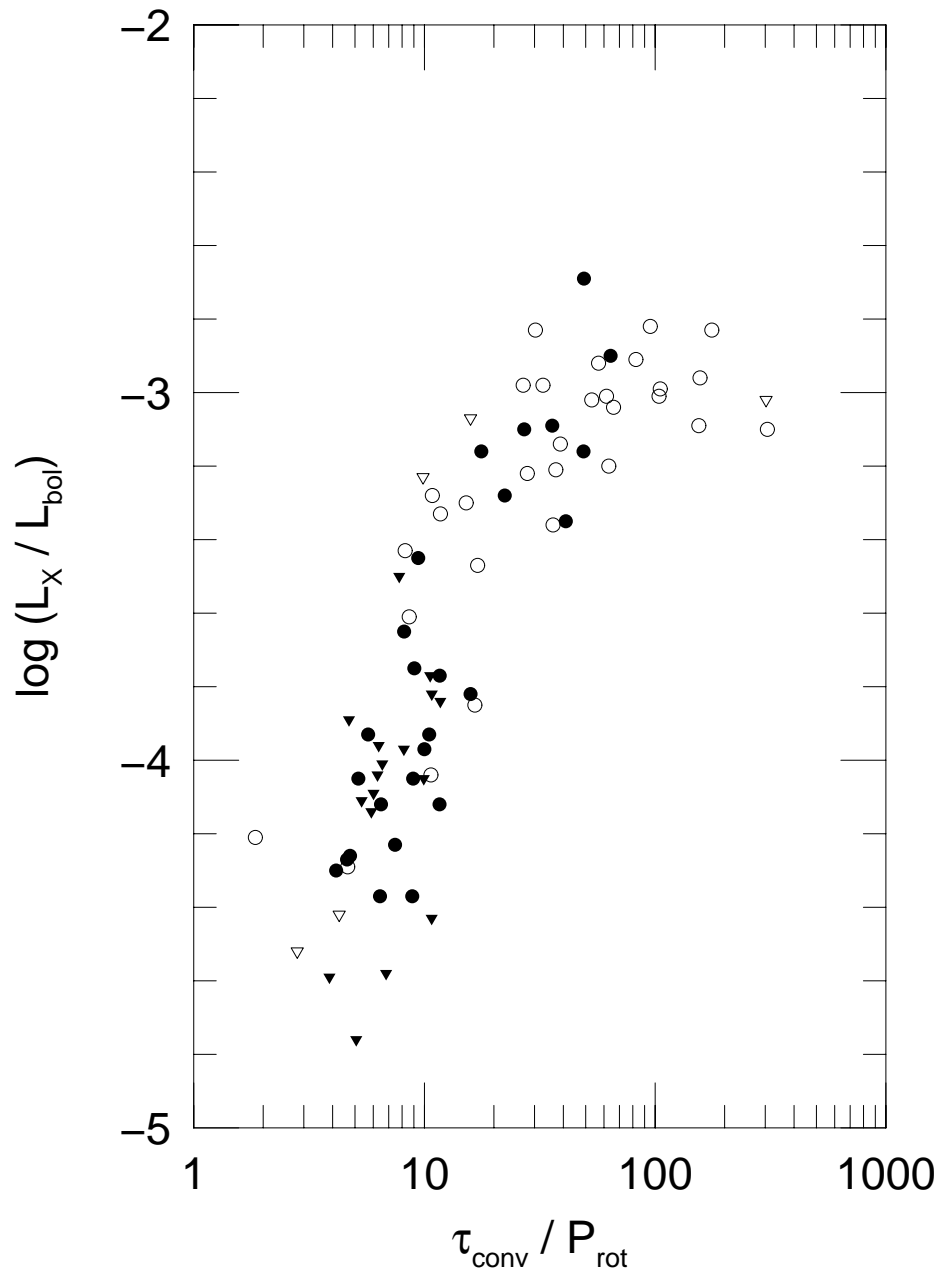


Fig. 7.— X-ray luminosity against inverse Rossby number. Solid points show stars in NGC 2516, while open points are Pleiades stars with measured periods. Triangles show upper limits. See text for details.

Table 1. NGC 2516 data

Star	Source	$v(r)$	$\sigma(v)$	$v \sin i$	σ	V	$B - V$	$V - I$	JTH	phot?
CTIO-1	2	24.2	1.0	≤ 8	...	14.701	1.014	1.094	6049	Y
CTIO-2	2	23.3	0.6	≤ 6	...	14.184	0.903	1.007	6263	Y
CTIO-3	2	24.7	0.6	≤ 6	...	14.287	0.938	1.007	6676	Y
CTIO-5	2	24.8	0.8	≤ 7	...	14.804	1.051	1.105	8654	Y
CTIO-6	2	22.1	1.6	11.7	3.0	13.590	0.779	0.889	9361	Y
CTIO-7	2	23.7	0.7	10.5	1.1	13.735	0.804	0.896	10753	Y
DK078	1	27.4	0.9	24.2	2.2	12.068	0.603	0.741	7864	Y
DK081	2	26.4	5.0	10.725	0.328	0.445	8058	Y
DK206	1,2	23.2	1.0	18.3	4.6	12.696	0.637	0.743	7967	Y
DK215	1	25.9	0.8	21.6	1.2	12.682	0.636	0.750	7104	Y
DK221	2	23.4	0.8	≤ 7	...	13.293	0.814	0.875	6880	Y
DK230	1	27.1	0.5	12.8	1.0	12.792	0.597	0.704	6700	N
DK232	3	24.2	0.6	10.0	7.0	11.370	0.386	0.474	6446	Y
DK233	1	22.8	0.6	12.6	1.0	12.240	0.674	0.769	6029	Y
DK234	1	20.0	0.7	9.2	1.2	13.661	0.874	0.987	5887	Y
DK245	1	24.8	0.4	9.5	1.1	13.541	0.768	0.853	4914	Y
DK307	3	21.2	2.1	73.8	1.6	11.753	0.499	0.625	7189	Y
DK308	1,2	23.9	1.3	10.5	1.6	13.047	0.684	0.794	6452	Y
DK311	1	24.0	3.1	37.7	3.7	12.437	0.602	0.718	5833	Y
DK313	1,2	24.8	0.9	15.4	1.3	13.289	0.732	0.843	5862	Y
DK320	1,2	24.8	0.8	13.7	1.1	12.878	0.675	0.818	3208	Y
DK323	1	23.7	0.8	22.6	2.1	12.503	0.592	0.701	3621	Y
DK325	1,2	23.3	0.5	11.6	0.8	13.020	0.671	0.762	4574	Y
DK403	1	30.4	1.2	26.3	1.7	12.905	0.719	0.876	7585	Y
DK409	2	22.5	0.7	≤ 7	...	13.730	0.809	0.907	6852	Y
DK415	2	24.8	1.5	15.3	2.4	12.954	0.671	0.800	5901	Y
DK428	1	22.2	0.5	16.4	0.7	13.312	0.751	0.924	4105	Y
DK463	2	25.5	0.6	7.5	1.0	13.399	0.742	0.873	6570	Y
DK513	1	23.5	1.2	24.4	2.1	12.647	0.655	0.802	7743	Y
DK514	2	24.1	0.6	≤ 7	...	13.839	0.831	0.922	7312	Y
DK526	1	24.9	1.1	25.4	1.9	12.759	0.649	0.778	6976	Y

Table 1—Continued

Star	Source	$v(r)$	$\sigma(v)$	$v \sin i$	σ	V	$B - V$	$V - I$	JTH	phot?
DK609	1	24.4	0.4	10.9	1.0	12.142	0.659	0.758	9852	Y
DK612	3	25.1	0.5	65.5	4.7	11.534	0.444	0.542	10301	Y
DK664	1	25.9	1.8	47.9	1.6	13.840	0.818	0.963	9465	Y
DK668	1	19.6	1.8	42.8	1.2	14.120	1.065	1.141	8645	Y
DK722	1	24.5	0.6	8.6	0.9	13.756	0.801	0.896	11716	Y
DK742	3	22.5	0.7	53.1	1.0	11.704	0.480	0.795	14681	N
DK803	2	23.2	1.1	16.4	2.2	13.405	0.736	0.838	9140	Y
DK820	1	22.6	0.4	9.7	1.2	14.279	0.934	1.085	12118	Y
DK875	3	25.6	1.3	108.8	8.4	12.000	0.526	0.647	12302	Y
DK902	2	20.8	5.0	11.465	0.533	0.665	8458	Y
DK904	1	27.6	1.0	22.6	1.0	12.841	0.691	0.836	9054	Y
DK907	3	25.1	1.0	24.4	0.5	12.336	0.583	0.709	8529	Y
DK908	2	24.7	0.7	10.1	1.1	12.871	0.660	0.760	8536	Y
DK914	2	24.5	0.6	9.1	1.0	13.641	0.780	0.851	9446	Y
DK933	1	23.1	0.5	14.1	0.8	12.607	0.762	0.864	9486	Y
E010	2	23.2	2.7	32.4	3.3	14.335	0.903	1.048	9676	Y
E020	1	25.1	0.4	9.7	1.3	14.322	0.935	1.008	7619	Y
E027	2	27.1	1.8	19.4	2.4	14.429	0.928	1.052	7678	Y
E063	1	24.9	0.4	8.7	1.1	14.509	0.976	1.061	10871	Y
E095	1	25.0	0.4	7.6	1.2	14.240	0.930	1.000	9286	Y
GSC89111169	1,2	22.1	2.7	38.5	2.9	14.516	0.943	1.118	8634	Y
GSC89111238	1	24.5	1.1	27.2	1.3	13.984	0.861	1.016	4598	Y
GSC89111475	1	24.6	1.2	37.1	1.4	14.576	1.015	1.080	5957	Y
GSC89113284	1	22.6	0.5	11.8	1.2	14.867	1.034	1.171	10040	Y
JTH 758	3	23.7	0.7	24.4	2.0	12.632	0.640	0.794	...	Y
JTH 14223	3	23.0	0.7	40.6	1.4	12.121	0.537	0.672	...	Y
Nonmembers										
DK306	1	82.0	6.9	53.1	2.5	13.747	0.726	0.856	7147	N
DK365	1	91.3	0.8	≤ 7.0	...	13.968	1.022	1.108	6705	Y

Table 1—Continued

Star	Source	$v(r)$	$\sigma(v)$	$v \sin i$	σ	V	$B - V$	$V - I$	JTH	phot?
DK417	1	9.0	1.1	17.9	1.4	12.053	0.515	0.619	6096	Y
DK503	1	65.6	1.9	32.4	3.4	12.706	0.620	0.768	7650	Y
DK508	2	43.6	2.6	126.3	5.2	11.250	0.376	0.456	6949	Y
DK573	1	0.8	0.7	≤ 7	...	14.380	0.874	1.048	6307	N
DK574	1	77.0	0.6	≤ 7	...	14.009	1.043	1.112	6724	Y
DK625	1	337.0	0.4	≤ 7	...	13.892	0.822	0.999	11031	Y
DK669	1	-0.4	0.5	≤ 7	...	13.933	0.966	1.046	8689	Y
DK813	1	38.3	0.5	8.8	0.5	12.029	0.654	0.980	10390	Y
DK919	1	13.8	0.3	7.3	1.3	14.215	0.950	0.982	8262	Y
DK967	2	56.0	0.5	10.0	7.0	12.164	0.546	0.745	12923	Y
E013	1	31.2	0.5	9.9	1.3	14.762	0.996	1.139	8967	Y
E111	1	5.1	0.5	≤ 7.0	...	14.037	0.817	0.979	6649	Y

Note. — Sources for the data: (1) Observations at CTIO (this study); (2) Jeffries et al. (1998); (3) Observations at AAT (this study).

Table 2. Cluster radial velocity

Sample	r.v. (km s ⁻¹)	<i>N</i>
All stars (this study)	24.2 ± 0.2	57
Jeffries et al. (1998)	23.8 ± 0.3	24
González & Lapasset (2000)	22.0 ± 0.2	22

Table 3. Error budget for main-sequence fit

Source of error	value	$\Delta(V_0 - M_V)$	$\Delta(\text{[Fe/H]})$
Fit to data points	...	± 0.015	± 0.02
Error in $E(B - V)$	± 0.02	∓ 0.020	± 0.10
Error in $E(V - I)/E(B - V)$	± 0.02	∓ 0.065	± 0.06
Total error	...	$\mp 0.14^a$	± 0.14

^aIncluding the effect of the abundance error, which is $\Delta(V_0 - M_V)/\Delta(\text{[Fe/H]}) = +1.3$.